[003]附属環境工学研究教育センター研究活動報告
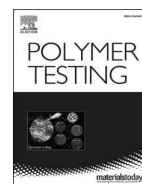
Study on the influence of inductive groups on the performance of carboxylate-based hydrogel polymer network

Nguyen Sura [a,b,*], Hirotaka Okabe [a], Brian A. Omondi [a], Albert Mufundirwa [c], Yoshiki Hidaka [a], Kazuhiro Hara [a,**]

[a] Department of Applied Quantum Physics and Nuclear Engineering, Faculty of Engineering, Kyushu University, 744 Motooka, Fukuoka, 819-0395, Japan
[b] Vietnam Petroleum Institute, 167 Trung Kinh, Yen Hoa, Cau Giay, Hanoi, 10000, Viet Nam
[c] Department of Mechanical Engineering, Faculty of Engineering, Kyushu University, 744 Motooka, Fukuoka, 819-0395, Japan

ABSTRACT

We report study on the effect of Br and CH_3 inductive groups on the loading capacity of carboxylate-based hydrogel adsorbent. Synthesized sodium acrylate (NaAc) and 2-Bromoacrylic acid (BrAc) copolymer hydrogels for metal ion capture were characterized using FTIR, UV–Vis, ^{13}C NMR, and DSC methods for structural and functional properties. Both FTIR and UV–Vis spectra indicated formation of a charge transfer complex between Br, CH_3 groups and the carbonyl ($C\!=\!O$) group whereas solid-state NMR evidenced Br group appearance as an appendage on hydrogel backbone. By incorporating Br group on the hydrogel matrix and consequently exploiting the high electronegativity potential and inductive effect chemistry of this group, there was a significant increase in dissociation of H^+ ions and hence higher loading capacity of carboxylate group. This facilitated higher ion exchange ability, resulting in up to 4 times increase in adsorption capacity during adsorption from multi-element metal ion competitive solution. Separately, when applied on single ion non-competitive solution, its adsorption capacity on vanadium increased three-fold from 119 mg/g to 373 mg/g due to the effect of Br group. However, the CH_3 had a negating effect instead lowering the adsorption capacity (below 119 mg/g); while also caused lower swelling ratio of carboxylate-functionalized hydrogel adsorbents.

1. Introduction

Hydrogel have emerged as among the ubiquitous adsorbents widely synthesized for applications in pollution control, or harvesting and recovery of rare earth valuable elements existing in trace quantities from seawater [1–5]. Adsorption using hydrogel material can be easily applied in low concentrations environments, compared to traditional separation method like chemical precipitation and solvent extraction. This is achieved using techniques like ion-exchange adsorption, but when the need for selectivity is paramount then molecular recognition technology via site selective functional groups is most suitable [6–9]. With such techniques, hydrogels are increasingly being considered as alternative candidate adsorbents capable of meeting pollution control limits and complete toxic metal ions removal, with very low energy demand and they do not produce harmful sludge, instead enabling recovery of adsorbed substrates [10,11].

Adsorption via ion exchange is still the most common technique, and in the case of hydrogels, acrylic acid based adsorbents are the most commonly fabricated for studies on decontamination of heavy metals [12]. Unique properties of acrylate hydrogels are based on two vital features of acrylic monomer: First, its vinyl property, whereby the acrylic monomer's double bond enables easy polymerization and crosslinking reactions to form 3D polymer network (i.e. a gel) with a mesh in nanometer-scale [13]. This vinyl property is paramount in gel fabrication studies. Secondly, the carboxylate functional group (−COOH) of the acrylate is hydrophilic in nature, and has comparatively high dissociation ability. Consequently, the H^+ ion concentration within acrylate hydrogel is greater than in surrounding solution. This prompts an imbalance in osmotic pressure and leads to a flux of solution into hydrogel, eventually promoting high amount of water uptake [14]. This way, acrylate hydrogels are super absorbents with high swelling ability. Further, high ionization also makes them good ion exchanger adsorbents

for use in hazardous metals ions decontamination [15–18].

However, the –COOH still faces many drawbacks as it is considered a weak polyelectrolyte, and that its degree of protonation is dominated by ionic repulsion and pH of test solution [19]. This is undesirable in practical industrial application due to the need for strenuous pH adjustments. Also, it has low chemical loading capacity, resulting in low effectiveness when used for metal ion capture from low concentration solutions (1–100 mg/L) [20]. Accordingly, many investigations have sought to optimize the structure-property relationships of the COOH functional performance. One such method has been through grafting of acrylic acid monomer onto existing organic or inorganic polymer backbones such as poly(tetrafluoroethylene) and lignin [21,22]; or also via copolymerization with other monomers possessing disparate functional groups such as amides or nitriles [23,24]. In both cases, grafting and copolymerization have aimed to increase the loading capacity and performance of the COOH by interacting it with different functional groups.

An interesting point has also been found that the number of functional sites is not very critical for increasing the loading capacity. Because in Hara et al. investigations [25], the metal ions removing capability of MA/AAm (maleic acid/acrylamide) hydrogel was lower than NaAc/AAm (sodium acrylate/acrylamide) hydrogel despite MA having more carboxylate groups (loading capacity) than NaAc. Instead, it is the dissociation degree, rather than the number of carboxyl-groups within hydrogels, that is important for increasing ion exchange –and hence metal capturing– ability.

Dissociation studies of COOH has been explored by Huglin et al. [26] who showed that hydrogels containing methyl group appendage demonstrated lower degree of dissociation such as the polymethacrylic acid (PMAA) hydrogel compared with polyacrylic acid (PAA) hydrogel. The degree of dissociation value for the former and the latter are 0.1 and 0.3, respectively. Implying that presence of the methyl group in PMAA possibly decreased the ionization capacity of the COOH group. Indeed, this effect is corresponding to the fact that electron attracting capacity of methyl group (2.30) is lower than carboxylic group (2.85). These results therefore suggested the influence of inductive groups on the performance of –COOH containing adsorbents could not be ignored. Therefore, if instead inductive groups with higher electron attracting capacity could be used, this would probably cause a positive influence on the degree of COOH dissociation, hence higher ion exchange capacity and consequently higher adsorption capacity of carboxylate hydrogel adsorbents. One such group is the Br, whose electronegativity is 2.96. Electronegativity values of various functional groups have been researched and listed by Mullay et al. [27]. From literature review, –Br function group has not yet been applied for acrylic hydrogel types to enhance metal recovery.

In the present contribution, we attempted to use different inductive groups (i.e. Br and CH_3 -based inductive groups) as co-monomers with sodium acrylate. This research aimed to find out the loading effect of these inductive groups on the ion exchange dissociation degree of carboxylate-based hydrogels. We investigated the role of matrix to the final activity of hydrogel behavior, especially the effect of increased/decreased electron density onto the COOH and the resultant contribution onto the hydrogel's adsorption capacity of selected metal ions from both competitive and non-competitive solutions. The study also explored the possibility of achieving selectivity with such hydrogels.

2. Materials and experimental methods

2.1. Chemical reagents used

Sodium Acrylate (NaAc), Sodium methacrylate (NaMAc), 2-bromoacrylic acid (BrAc) and polymerization agents: ammonium persulfate (APS), *N, N′*-methylenebisacrylamide (BIS) and *N,N,N,N*-tetra-methylene diamine (TEMED) were all supplied from Sigma-Aldrich. The main solvent was water and dimethylsulfoxide (DMSO) solution obtained

from Wako chemicals (Japan). For adsorption testing, a multi-element metal ion stock solution (ICP/MS standards) and test solutions of Zn^{2+}, Cu^{2+}, Co^{2+}, Fe^{3+}, Cr^{3+}, and VO_2^+ were obtained from Sigma-Aldrich (Japan). All chemicals used as received and were of analytical grade. References to water shall refer to the ultrapure deionized water.

2.2. Preparation of hydrogel

Two types of hydrogels were synthesized via standard radical polymerization method. The first hydrogel aimed to find out the effect of a negative inductive group (Br group) onto the carboxylate functionality. To do this, BrAc was used as co-monomer with NaAc in several ratios (under the condition of [BrAc] + [NaAc] = 1.0 M) as illustrated in Table 1. The monomers were dissolved in 10 mL aqueous DMSO solvent (5% v/v) to make the pregel solution. Thereafter, 40 mM of BIS cross-linking agent was added to facilitate 3D network formation, together with 20 mM of TEMED reaction accelerator. Polymerization process was initiated using 10 mM of APS free-radical initiator polymerization and the final pregel solution incubated at 40 °C isothermal water bath for 24 h until complete gelation (Fig. 1(a)). In a similar manner, the second type of hydrogels designed with positive (CH_3-containing) inductive groups were prepared using NaMAc as co-monomer with NaAc to give total concentration of [NaMAc] + [NaAc] = 1.0 M (Fig. 1(b)). Three subtypes of yNaMAc hydrogels (where y = % mole) were prepared as indicated in Table 1. This Table also highlighted that the limiting solubility of Br– and CH_3– groups in aqueous DMSO implied that only up to 15% for BrAc and up to 70% for NaMAc could be used as co-monomers with NaAc.

Finally, control sample hydrogel with only NaAc as sole monomer was synthesized in a similar manner using BIS cross-linking agent, APS reaction initiator and TEMED reaction accelerator. Following successful syntheses of the three types of hydrogel adsorbents, the gels were extracted from the synthesis vessels and cut into ~10 g cube fractions. Immediately, the hydrogels fractions were activated by washing extensively in ultrapure water to ensure all non-reacted components were dissolved and removed, such that only the cross-linked, insoluble material would remain. The activated hydrogels were then dried, characterized and tested for adsorption properties.

2.3. Physico-chemical characterizations

2.3.1. Swelling experiments

Swelling via water intake is a critical and unique property of hydrogels since water is the main solvent harboring heavy metal pollutants. Therefore through swelling, water could be used as a carrier to transport the dissolved heavy metals into the interior network of hydrogels, and consequently increase the adsorption capacity. Prolonged water immersion is also used to test the insolubility of the hydrogel and confirm its suitability as an adsorbent for such conditions.

For the actual swelling experiments, 0.5 g of each type of (dried, activated) hydrogel was immersed into beakers full of water. At respective pre-determined time intervals, the hydrogels were extracted, dried and their swollen masses recorded. This was repeated until the maximum swelling capacity was attained (12 h) beyond which there was no change in mass. The swelling factor was calculated based on equation

Table 1
Nomenclature of prepared hydrogels.

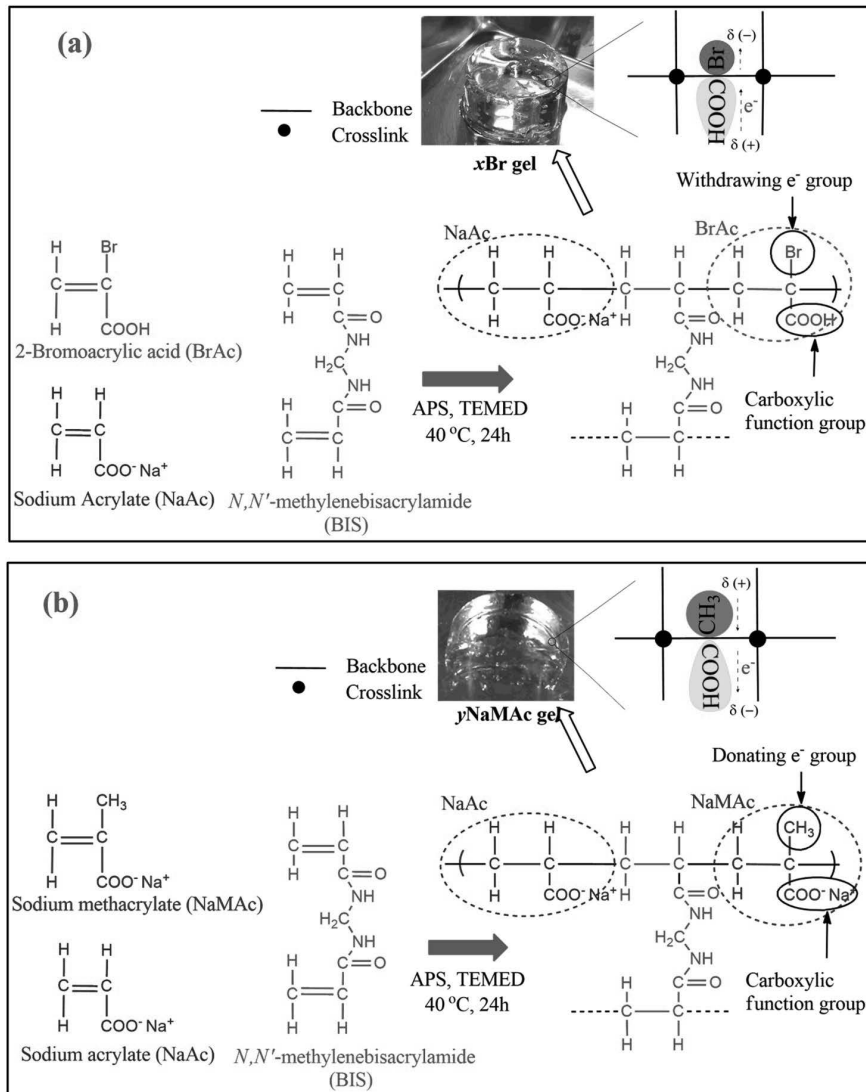| Composition (%mole)	Abbreviation
100% NaAc	NaAc
5% BrAc; 95% NaAc	5 Br
10% BrAc; 90% NaAc	10 Br
15% BrAc; 85% NaAc	15 Br
30% NaMAc; 70% NaAc	30 NaMAc
50% NaMAc; 50% NaAc	50 NaMAc
70% NaMAc; 30% NaAc	70 NaMAc

Fig. 1. Schematic outline on the formation of (a) xBr hydrogel, and (b) yNaMAc hydrogel.

(1),

$$S.F = \frac{(M_s - M_d)}{M_d} \qquad (1)$$

where $S.F$ is the swelling factor, M_s (g) is the mass of the swollen hydrogel, and M_d (g) is the mass of the dry hydrogel.

Swelling investigations also aimed to determine the mechanical stability of the hydrogels. To do this, once the maximum swelling time and mass was determined, the hydrogels were dried until constant dry weight. The dry hydrogels were then re-immersed into water until maximum swelling was attained, and the equilibrium mass confirmed before the swollen hydrogels were then dried again. This cycle of swelling-drying-swelling was repeated 3 times in order to ascertain if the gels retained their structural consistency upon several re-use cycles (Fig. 2).

2.3.2. Thermal stability

Pyrolysis experiments were used to study the stability of the synthesized hydrogels under imposed high thermal conditions. Each of the three hydrogels was ground into powder form of ~500 μm size in order
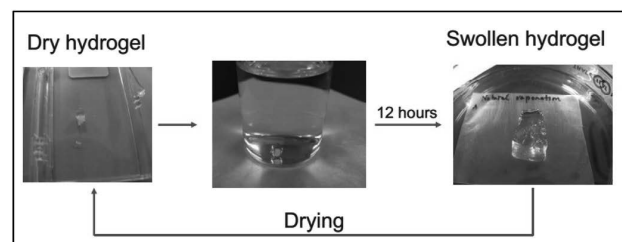

Fig. 2. Swelling and drying experiment to ascertain hydrogel structural stability.

to avoid overheating. Then using the TG-DSC (NETZSCH, Japan) simultaneous STA 449 F3 thermal analyzer, hydrogel pyrolysis was then conducted under N_2 atmosphere at $10\,°C/min$ following by $5\,°C/min$ and analyzed up to $550\,°C$. Obtained results were interpreted using differential thermal analysis (DTA) and weight loss derivative (DTG) curves as a function of time and temperature. An outline of this investigation has been summarized in Fig. 3.

3

2.3.3. Functional groups characterization

Examination of carboxyl functional group and confirming the incorporation of inductive group including CH_3- and $Br-$ group into the hydrogels matrix were conducted applying Jasco 4100 FT/IR spectroscopy. Prior to FT/IR analysis, the samples were maintained at 60 °C elevated temperatures for 36 h and later dried for 10 days in order to minimize the effect of bound water.

Meanwhile the change in the electron density of the functional group was investigated by UV–Vis spectrometer (USB4000 Ocean Optics, USA). Different thin sliced samples were prepared for measurement. Data was collected between the wavelengths of 200 nm and 420 nm with the path length of 3 mm for thin gel sample that were swollen water. Deionized water (pH 7.0) was used as a baseline. The procedure was carried out at ambient temperatures.

However, since FTIR and UV–Vis cannot directly detect the presence of $Br-$ group, we performed ^{13}C NMR examination using CPMAS (Cross Polarization Magic Angle Spinning) technique with aim of identifying the types of carbon and carbon environments in gel sample [28].

2.4. Batch adsorption experiments

The metal adsorption performance of the three different types of hydrogel containing either $Br-$ group, $-CH_3$ group and without inductive group was investigated. The hydrogel activity was tested in both competitive and non-competitive metal ion solutions using common metal ions popular to electroplating or other heavy metal related factories (Zn^{2+}, Cu^{2+}, Co^{2+}, Fe^{3+}, Cr^{3+}, VO_2^+). In all cases, the volume of metal analyte solution used was 0.025 L at un-adjusted pH of 2.1, whereas the amount of hydrogel adsorbent had a corresponding to dry mass of approx. 1.3×10^{-3} g. The pH was maintained at low acidic levels in order to test the adsorbents effectiveness at this low pH where most metal ions in waste solutions usually exist.

In the first step, the inductive group effect on hydrogel performance was investigated under competitive environment. An integrated multimetal ion solution comprising Zn^{2+}, Cu^{2+}, Co^{2+}, Fe^{3+}, Cr^{3+}, and VO_2^+ metal ions was prepared, with each metal concentration of 50 mg/L within the single solution. Subsequently, hydrogel pellets of BrAc, NaMAc and NaAc hydrogels were immersed into vials containing 0.025 L volume of the multi-ion competitive solution for the actual batch adsorption, carried out under constant agitation of 110 rpm to ensure homogeneous surface adsorption. Adsorption was repeated with different ratios of inductive group hydrogels, and all investigations were performed at ambient conditions.

Additionally, single ion non-competitive adsorption was explored, whose results were intended to eventually be applied against uranium adsorption and recovery. Consequently, vanadium was used as surrogate for uranium due to the similarity between the two metals. Single ion

solutions of vanadium were prepared at 50 mg/L concentration and for each batch; a volume of 0.025 L was used, whereas the pH was unaltered at pH 2.1. BrAc, NaMAc and NaAc hydrogels were immersed into this solution for batch adsorption, performed under similar conditions as multi-metal solution. At these conditions of pH and concentration, vanadium exists as VO_2^+ as predicted by Sadoc et al. in their analysis of $logC_v$ – pH of this metal ion [29].

In both cases, adsorption was allowed for 2 days until equilibrium capacity. Thereafter, for each batch, changes in metal ion concentrations due to hydrogel adsorption were measured and analyzed using inductively coupled plasma mass spectrometer (ICP/MS, Agilent 7700X, Japan). The results were utilized to calculate the metal adsorption capacity, q (mg/g) as follows:

$$q = \frac{(C_i - C_f)V}{m} \tag{2}$$

where q (mg/g) is the material adsorption capacity, V (L) is the volume of the metal ion solution, m (g) is the mass of dried hydrogel, C_i and C_f (mg/L) are the initial and residual metal ions concentrations in feed solution before and after sorption, respectively.

The performances of the three adsorbents were analyzed to estimate the effect and suitability of the types of inductive groups in enhancing ion exchange functionality.

3. Results and discussion

3.1. Physico-chemical properties

3.1.1. Fourier transforms infrared (FTIR)

Fig. 4 presented the FTIR spectra of the carboxylate-functional hydrogels incorporated with inductive groups, (a) xBr and (b) yNa-MAc hydrogels. For comparison, a reference spectrum of sample without inductive group (NaAc) was included in each graph. As shown in Fig. 4 (a), primary carbonyl group (C=O) stretching in reference sample displayed two well-defined peaks at 1550 and 1650 cm^{-1} due to hydrogen bonded dimeric and monomeric state. But upon introduction of Br group, a new shoulder absorption peak of C=O vibration appeared at 1752 cm^{-1}. The intensity of this peak increased as Br concentration increased from 5 to 15% (i.e. BrAc:NaAc = 5/95 to 10/90 to 15/85). This peak was most likely due to the Fermi resonance synergy between the first overtone and the normal vibration of C=O stretching in presence of $Br-$ group [30]. Also in Fig. 4(b), the 950 cm^{-1} peak was assigned to the rocking mode of $-CH_3$ group [31]. In a similar way to the previous Br effect on C=O group, the intensity of $-CH_3$ peak becomes higher with increasing NaMAc ratio.

Other FTIR spectral assignments included the C–H vibration (2930 cm^{-1}) and O–H vibration at 3000 to 3500 cm^{-1}. Conclusively, the

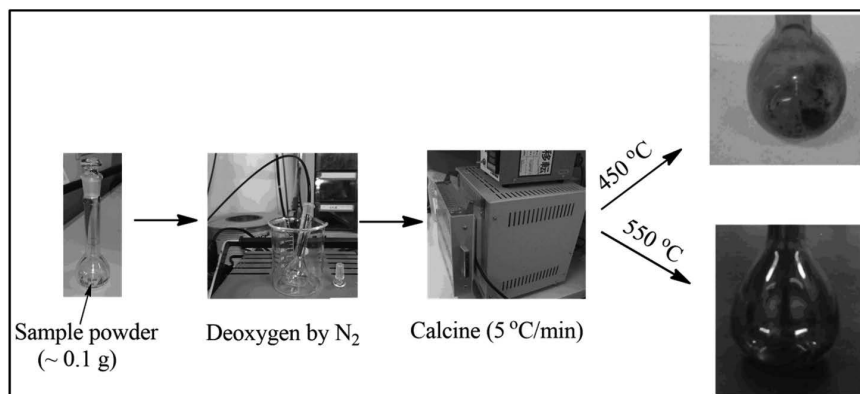Sample powder (~ 0.1 g) → Deoxygen by N₂ → Calcine (5 °C/min) → 450 °C / 550 °C

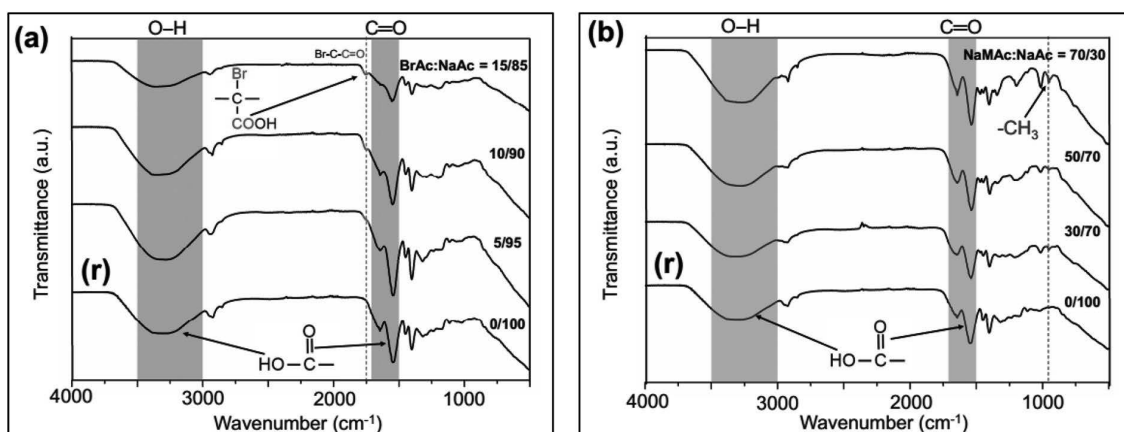**Fig. 3.** Process for the xBr hydrogel pyrolysis.

Fig. 4. FT-IR spectra of (a) xBr hydrogels (BrAc/NaAc = 5/95, 10/90, 15/85) and (b) yNaMAc hydrogel (NaMAc/NaAc = 0/100, 30/70, 50/70, 70/30) (r) reference sample.

FTIR spectroscopic results provided concrete evidence about the presence of –COOH in all three hydrogels, in addition to −Br, –CH$_3$ group for xBr and yNaMAc hydrogels, respectively.

3.1.2. UV–vis spectral

Further, to confirm the incorporation of –Br, –CH$_3$ group on the hydrogel matrix, UV–visible absorption studies were carried out. In Fig. 5, a strong representative absorption peak around 230 nm on the reference sample NaAc gel was likely from the chromophore absorbing of carbonyl group (−C═O). The moving of two lone pairs electron in 2s and 2p orbital of oxygen atom from normal state (n) to antibonding state (π*) was responsible for this n–π* transition.

Meanwhile, in xBr gel, the generation of a charge transfer complex between the carbonyl (C═O) group and Br− will display a hyper chromic phenomenon when one pair of non-bonding electrons of –Br group can interact with the π electrons. This will cause stabilization of the π* state and the electron transition from n → π* orbital then requires less energy [32]. Consequently, as illustrated in the UV-spectrum, the absorbency peak of xBr gel would be two times higher than in the reference gel.

But for yNaMAc gel, the methyl inductive group (−CH$_3$), also known as an auxochrome group, has hyperconjugation effect between the σ electrons of the alkyl group and the chromophoric group (C═O). This would provide additional opportunity for charge delocalization and thus
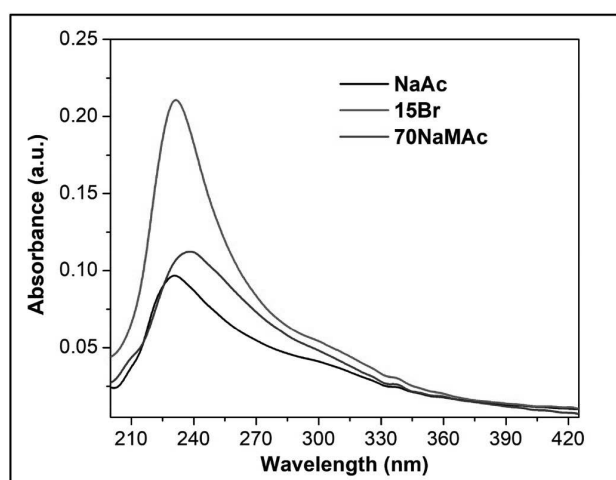
lower energy for transition to excited states, than for xBr gel. As a result, the excitation absorption peak wavelength for yNaMAc was lower and slightly shifted towards longer wavelength of 238 nm (instead of 230 nm).

3.1.3. NMR analysis

The ^{13}C NMR spectra of 15Br gel presented in Fig. 6 showed five distinctive ^{13}C NMR peaks, appearing at chemical shift values 185 ppm, 178 ppm, 87 ppm, 45 ppm and 41 ppm respectively. In analyzing these results, the most downfield chemical shifts at 185 ppm and 175 ppm were likely from sp^2 hybridization (sp^2 carbon) emanating from carbonyl carbon. This carbon was also previously identified in the FTIR results in Fig. 4 where we had isolated –COOH as the main functional group of xBr hydrogel. Therefore identification of carbonyl carbon confirmed the presence of carboxylate in xBr hydrogel. The duality of this peak at both 185 ppm and 175 ppm was likely due to different chemical environments as summarized in the inset of Fig. 6, where there was additional withdrawal effect of Br on one carbonyl carbon, which was absent in the other. Separately, other peaks at upfield ends appeared in the zone of alkyl carbons, and could then distinguished by the nature of deshielding effect. Such that the least deshielded equivalent carbon would appear at upfield end (41 ppm) whereas the most deshielded 4° carbon would resonate at region of downfield end (87 ppm) due to electron withdrawing effect of Br. These results strongly confirmed the presence of carboxylic function group and Br− group on the main
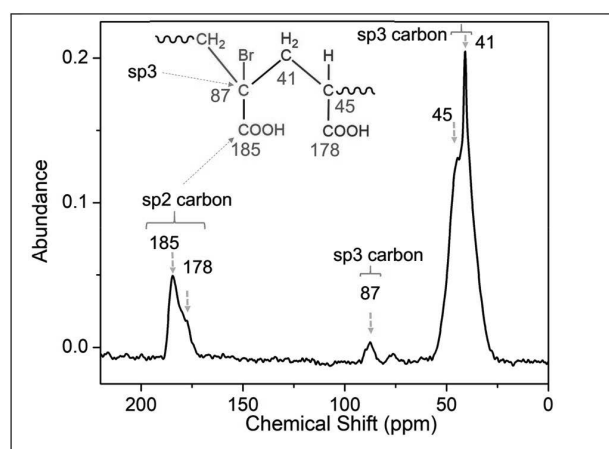

Fig. 5. UV–Vis spectra of 15Br gel, 70NaMAc gel and NaAc gel.

Fig. 6. ^{13}C NMR spectral shift of modified carboxylate hydrogel.

5

backbone of xBr gel network structure.

3.1.4. Thermo-physical analysis

Analytical hydrogel decomposition aimed to retrospectively collect information on the macromolecule by pyrolyzing and identifying the products of thermal degradation. We studied the decomposition of xBr gel using differential thermal analysis (DTA) and performed weight loss derivative curve (DTG) measurements. Thermal stability was estimated by comparing decomposition temperature with yNaMAc gel, which is a widely studied gel containing electron donating group [33].

DTA thermograms of hydrogel are presented in Fig. 7 which revealed that in the gels with maximum concentration of –CH$_3$ or –Br inductive groups, the decomposition of 70NaMAc hydrogel started at 420 °C but only 380 °C for the 15Br hydrogel. The former was therefore more stable than the latter. One of the prime considerations governing thermal stability is the strength of the bonds in the molecule [34]. The C–Br bond, which exist on the backbone of the chain, is one of the weakest single bonds than the C–H bond, thus the xBr gel was expectedly less thermally stable than yNaMAc gels. The experimental and theoretical determinations indicated a value of 47.5–56.2 kcal/mol for the dissociation energy of the C–Br bond [35,36], against 116.3–131 kcal/mol for the C–H bond scission [37,38]. Since the decomposition of the C–Br unit occurred at high temperatures (over 350 °C), this attested to the thermal tolerance and stability of this group if lower temperatures would be used, such as room temperatures, which was the prevailing condition in all adsorption experiments.

Looking at the weight loss derivative curve (DTG, mg min^{-1}) in Fig. 7, decomposition could be described in three stages: the first stage was dehydration which occurred between 50 and 250 °C; followed by decarboxylation step between 300 °C to 380 °C temperatures and lastly the material decomposition at temperatures in excess of 380 °C. From these thermal treatment and degradation analysis results, we were able to learn that our material was mainly carboxylate-based hydrogel adsorbent, whose thermal tolerance could be raised by addition of –CH$_3$ containing groups, or lowered if instead –Br containing groups were incorporated into the hydrogel matrix. In other words, if application will be in high temperature environments, then higher methylated gels (70 NaMAc gel) or low brominated-gels (10Br gel) would be ideal. But it is imperative to first test the actual performance of these hydrogels on metal adsorption. This was undertaken via batch adsorption studies from concentrated metal ion solutions.

3.2. Hydrogel loading and functional group testing

3.2.1. Competitive adsorption

Initially adsorption was tested against a customized integrated multi-metal ion solution containing six metal ions. To eliminate any undue effects, it was ensured that the concentration of each metal ion within the solution was the same, whereas their ionic charge was an intrinsic property and ranged between +2, +3 and + 5 for the various ions. Of the three types of hydrogels investigated (i.e. NaAc gel, xBr gel and yNaMAc gel), adsorption results in Fig. 8 showed that it is the xBr gel that yielded the highest amount of metal adsorption.

The NaAc gel, acting as control sample, only contained the COOH functional groups as active sites and was able to adsorb 1415 mg/g of metal ions from the solution. But as the Br inductive group was gradually incorporated into the adsorbent to form the xBr gel, there was a significant increase in degree of adsorption. Initially in 5Br gel, the adsorption capacity increased 2.5 times compared to NaAc gel, and this increase continued linearly as the amount of Br inductive group was increased, until optimum capacity in 15Br gel to achieve $q = 5343$ mg/g. Thus, it was deducible that under optimum conditions, the Br group leads to four times increase in the performance of the carboxylate, which was a remarkably higher improved efficiency. Conversely, the methyl inductive group demonstrated a negative effect on the performance of the carboxylate. In Fig. 8 it was evident that as the methyl group increased from 30NaMAc to 70NaMAc, there was corresponding decrease in adsorption performance, which was even much lower than in the NaAc control adsorbent, which had no inductive group.
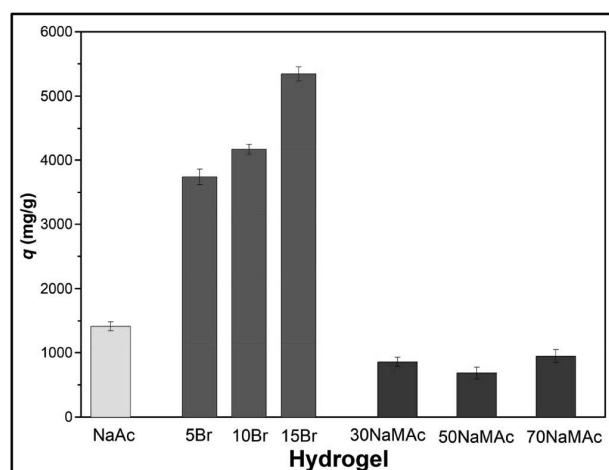
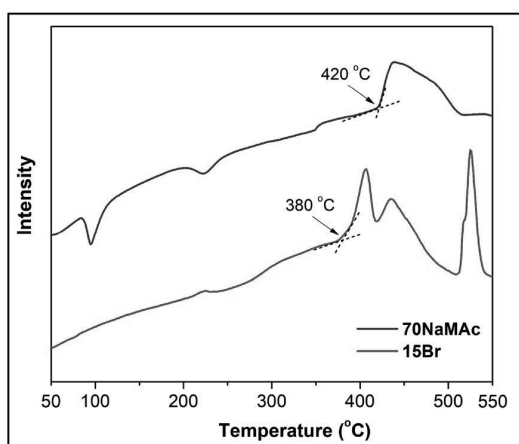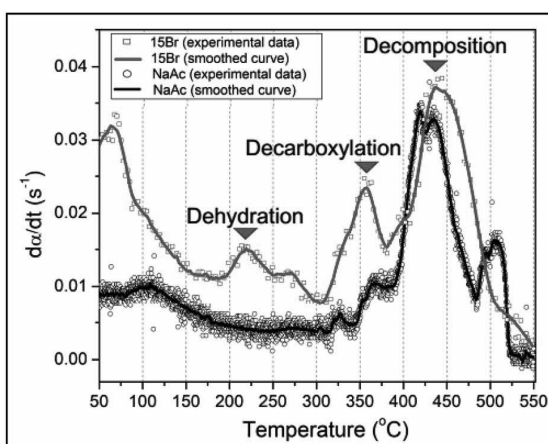Fig. 8. Adsorption capacity of 6-component ion aqueous solution onto NaAc, xBr and yNaMAc hydrogel adsorbents.

Fig. 7. DTA curves of 15Br gel and 70NaMAc gel; and the DTG weight loss derivative curves for NaAc gel and 15Br gel, respectively.

These results highlighted the influence of the inductive groups in promoting the ion exchange capacity. The Br inductive group possessing a high electronegativity factor caused a withdrawal of the electron density from the COOH, and corresponding increase in the positive charge on hydrogen of the carboxylate. The O–H bond became weaker, increasing the dissociation ability of the H^+ from the COO^- in the hydrogel matrix, thereby enabling easy release of H^+. With this high degree of ionization, it becomes easier for metal ions in solution to easily move from solution onto the adsorbent surface and exchange with carboxylate cations. Ultimately, there was a recorded high adsorption capacity via ion exchange when using xBr gels. But the results of the yNaMAc gels showed that effect of –CH_3 inductive group was contrary. This is due to the high electropositivity (low electronegativity) of –CH_3 which implied that the methyl appendages hindered the dissociation ability of the carboxylate cations, thus minimizing the ion exchange ability of these COOH functional groups with the metal ions in solution. This is what contributed to the observed low adsorption capacities in Fig. 8.

Further, a closer analysis of individual metal ion adsorption ratios by the xBr gel was summarized in Fig. 9 whence we can see that for each metal ion, there was simultaneous increase in degree of adsorption with increasing Br group concentration within the gel. The results also showed that the highest performing metal ion was Zn in all categories; however, there was no stand-out selectivity property with this adsorbent material. The lack of selectivity was attributed to the absence of a functional group or unique gel network design that would have promoted biased tendencies towards one ion compared to the others based on each distinct inherent characteristics. But with only COOH as the main functional groups, these groups are wholly dedicated to adsorb only via ion exchange, hence adsorption would only take place on these exchange sites, and will only be based on the oxidation number of the metal ion substrates. Therefore instead of selectivity, the individual adsorption capacities would only be distinguished based on charge density and Fig. 9 showed that Zn and Fe recorded the highest q values, hence highest charge densities, respectively, for higher ion exchange-ability. However, the authors caution that this was not a general trend, since some metal ions with higher charge densities like Fe^{3+} and Cr^{3+} recorded lower adsorption capacities than expected.

3.2.2. Non-competitive adsorption

Meanwhile, the performance of three hydrogels was also tested for adsorption from single metal ion solution (non-competitive conditions). After demonstrating the improved ion exchange capacity via effect of inductive groups, it is ultima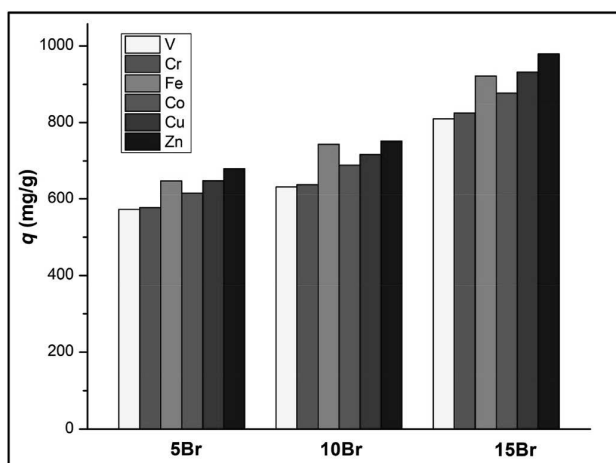tely intended that the best hydrogel adsorbent should be proposed for application in uranium harvesting as a natural resource, from seawater harvesting. Accordingly, in the present case vanadium was used as a surrogate for uranium during the adsorption experiments due to similarity between the two ions. Hydrogel adsorption results from vanadium non-competitive solution in Fig. 10 showed a similar trend to the previous performance against multi-ion competitive solution. The xBr hydrogels were the highest performing, followed by the control sample (NaAc gel), whereas the yNaMAc gel with methyl inductive groups was the least performing. The degree of yNaMAc gel performance was inverse to the amount of methyl group within the gel. Additionally, the results in Fig. 10 revealed that the actual adsorption capacities of single ion adsorption were significantly lower than in multi-element solution, by a factor of 10, in all categories of hydrogel. Nevertheless, these performance metrics demonstrated that 15Br hydrogel was the most ideal for application on maximum metal ion adsorption from both competitive and non-competitive solutions.

According to studies by Yi et al. [39] and Zhou et al. [40] dealing with polyacrylic acid hydrogel, cellulose-graft-acrylic acid hydrogels respectively, we can propose that the number of active sites of the reference NaAc copolymer hydrogel ranged between 1.1×10^{21} to 2.4×10^{21} mol active sites/g dry absorbance. The number of carboxylate active sites was obtained by molar ratio of the adsorption capacity of vanadium multiplied by the Avogadro number as shown in equation (3):

$$A = \frac{q}{M} \times 10^{-3} \times 6.02 \times 10^{23} \qquad (3)$$

where A = active sites q = adsorption capacity (119 mg/g); M = molar mass of vanadium. Therefore, in the present study it could be estimated that the amount of active site in NaAc gel was approximately 1.4×10^{21} mol active sites/g dry adsorbent. This figure would be higher in xBr gels since the latter was a co-monomer material hence possessed additional carboxylate functional groups. By incorporating Br inductive group, nearly all these active sites (per gram of dry adsorbent) could be able to participate in the ion exchange adsorption compared to when there is lack of Br group. This increased ionization capacity greatly escalated ion exchange adsorption of the metal ions as demonstrated in Figs. 8–10.

3.2.3. Effect of swelling ratio

The swelling property also played a critical role in influencing the nature of adsorption capacity of the hydrogels. Fig. 11 showed that whereas swelling was lower for methyl-containing gels, but the dry NaAc gel was able to swell 300 times its initial mass when placed in
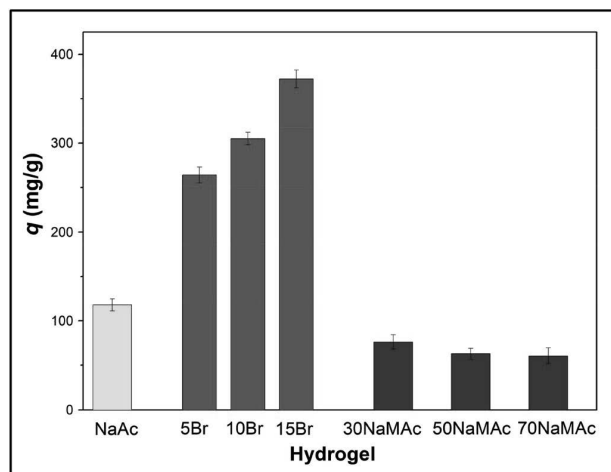

Fig. 9. Adsorption capacities of individual metal ions by xBr gel from competitive solution.

Fig. 10. Adsorption capacities of vanadium ions onto NaAc, xBr and yNaMAc hydrogel adsorbents.

water; and the swelling factor was significantly higher in xBr gels reaching up to ×1200. This highlighted the superabsorbency nature of these hydrogels, and further pointed out that only a small amount of material could then be used as adsorbent in aqueous solutions. Secondly, as the hydrogel swells, it increases in size and this also exposes the interior networks (and consequently exposes the hitherto hidden COOH groups) that otherwise would not have been accessed in non-swelling adsorbents. Thus, swelling facilitates adsorption on both the exterior surface active sites and the interior active sites, thus ensuring maximum adsorption on all the available active sites per gram of adsorbent. Additionally, since hydrogels imbibe water during swelling, and water is the main solvent for the dissolved metal ions, thus water also acts as a transport channel enabling the dissolved metal ions to access the interior network active sites of the adsorbent, for ion exchange adsorption. All these phenomena highlight the significance of swelling in adsorption investigations, and why hydrogels are increasingly becoming choice adsorbents compared to other materials.

3.3. Desorption and re-use

The main adsorption mechanism was via cation exchange between the hydrogel's carboxylate cations and the metal ion in solution. Therefore, in order to desorb and regenerate the adsorbent for potential re-use, conventional method is to immerse the metal-laden adsorbent into 5% nitric acid solution for extended period (24 h) under mild agitation [6,28]. All the metals will be eluted from adsorbent surface into the nitric acid solution, whereas the adsorbent would be regenerated with H^+ ions.

Additionally, as had premised previously during swelling investigations, it was important to ascertain the mechanical stability of the hydrogel structure in order to confirm its re-use potential. The hydrogels were tested through swelling/drying cycles described in Fig. 2 to confirm that its structure does not breakdown and to what level does the swelling ration remain consistent. The results showed that with up to 3 cycles, all the three types hydrogels comfortably swell and recovered their shapes and structure, with no loss in swelling efficiency upon re-swelling. Beyond this, however, the swelling efficiency decreased by 10% and 17% on the fourth and fifth cycles, respectively. The xBr gel was the most significant in achieving high adsorption results. Therefore for this type of inductive-modified hydrogel, adsorbent regeneration in nitric acid and re-use for adsorption experiments is proposed for up to 3 cycles, especially for 15Br gel whose structure was the least stable due to high amount of Br group.

4. Conclusion

In the present study, the authors proposed to find out the effect of bromine ($-Br$) and methyl group ($-CH_3$) as inductive groups grafted onto the hydrogel matrix towards increasing the loading capacity of the COOH functionality. Spectroscopic techniques showed that by using sol-gel method, the $-COOH$, $-Br$ and $-CH_3$ were successfully incorporated onto the hydrogel. This could also be identified retrospectively by analytical hydrogel decomposition. For demonstrating the effect of inductive group to higher functionality of hydrogels, tests for sorption of single ions and multi ions aqueous metal solutions were performed. In the actual batch adsorption analyses, $-Br$ group was found to be highly effective in raising the dissociation degree on the carboxylate ion exchange functionality. The metal adsorption capacity increased significantly with increasing $-Br$ group concentration, showing that $-Br$ inductive group had a much greater and positive inductive effect on increasing the loading capacity of the carboxylate than the $-CH_3$ group. These results on Br-grafted hydrogel toward heavy ion metal adsorption highlighted a notable potential for using other electronegative groups such as F, and Cl, to increase the loading capacities of ion exchanger adsorbents and promote higher metal adsorption capacities. Thus, the efficiency of such systems would be greatly improved.
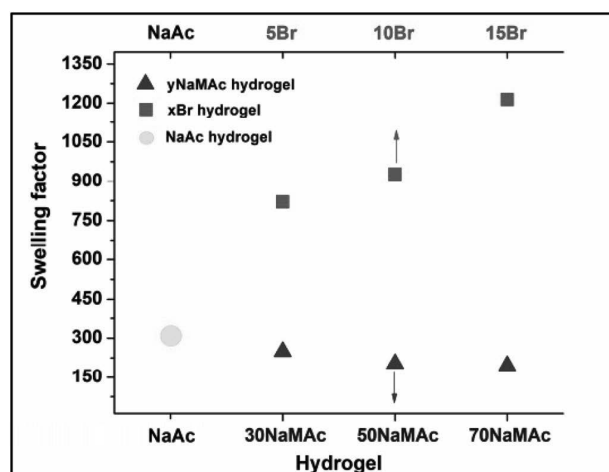

Fig. 11. Swelling ratios of NaAc gel, xBr gel and yNaMAc gels in water.

References

[1] F. Zhu, et al., Dual-responsive copolymer hydrogel as broad-spectrum adsorbents for metal ions, Polym. Test. 77 (2019) 105887.

[2] B. Sharma, et al., Nanomechanical analysis of chemically reduced graphene oxide reinforced poly (vinyl alcohol) nanocomposite thin films, Polym. Test. 70 (2018) 458–466.

[3] K. Hara, et al., Attempts to capturing ppb-level elements from sea water with hydrogels, Prog. Nucl. Energy 92 (2016) 228–233.

[4] K. Hara, S. Yoshioka, T. Nishida, A possibility of heavy-metal recycling by utilizing hydrogels, Trans. Mater. Res. Soc. Jpn.. 35 (3) (2010) 449–454.

[5] E.M. Ahmed, Hydrogel: preparation, characterization, and applications: a review, J. Adv. Res. 6 (2) (2015) 105–121.

[6] B.A. Omondi, et al., Fabrication of poly (1, 4-dioxa-7, 12-diazacyclotetradecane-8, 11-dione) macrocyclic functionalized hydrogel for high selective adsorption of Cr, Cu and Ni, React. Funct. Polym. 130 (2018) 90–97.

[7] B.A. Omondi, et al., Synthesis and characterization of poly (1, 4, 7-trioxacycloundecane-8, 11-dione) macrocyclic functionalized hydrogel for high selectivity adsorption and complexation of bismuth ion, Polymers 10 (6) (2018) 662.

[8] S. Çavuş, et al., The preparation and characterization of poly (acrylic acid-co-methacrylamide) gel and its use in the non-competitive heavy metal removal, Polym. Adv. Technol. 20 (3) (2009) 165–172.

[9] B.A. Omondi, et al., Multicomponent adsorption of benzene and selected borderline heavy metals by poly (butadiene-co-acrylic acid) hydrogel, J. Environ. Chem. Eng. 4 (3) (2016) 3385–3392.

[10] M.A. Barakat, N. Sahiner, Cationic hydrogels for toxic arsenate removal from aqueous environment, J. Environ. Manag. 88 (4) (2008) 955–961.

[11] V. Van Tran, D. Park, Y.-C. Lee, Hydrogel applications for adsorption of contaminants in water and wastewater treatment, Environ. Sci. Pollut. Control Ser. 25 (25) (2018) 24569–24599.

[12] M. Irani, H. Ismail, Z. Ahmad, Preparation and properties of linear low-density polyethylene-g-poly (acrylic acid)/organo-montmorillonite superabsorbent hydrogel composites, Polym. Test. 32 (3) (2013) 502–512.

[13] A. Pourjavadi, M. Kurdtabar, H. Ghasemzadeh, Salt-and pH-resisting collagen-based highly porous hydrogel, Polym. J. 40 (2) (2008) 94.

[14] Z. Fahimi, et al., Synthesis of pH sensitive hydrogels based on poly vinyl alcohol and poly acrylic acid, Iran. J. Pharm. Sci. 4 (4) (2008) 275–280.

[15] A. El-Hag Ali, et al., Synthesis and characterization of PVP/AAc copolymer hydrogel and its applications in the removal of heavy metals from aqueous solution, Eur. Polym. J. 39 (12) (2003) 2337–2344.

[16] R.D. Porasso, J.C. Benegas, M.A. van den Hoop, Chemical and electrostatic association of various metal ions by poly (acrylic acid) and poly (methacrylic acid) as studied by potentiometry, J. Phys. Chem. B 103 (13) (1999) 2361–2365.

[17] C. Morlay, et al., Potentiometric study of Cd(II) and Pb(II) complexation with two high molecular weight poly(acrylic acids); comparison with Cu(II) and Ni(II), Talanta 48 (5) (1999) 1159–1166.

[18] C. Heitz, J. François, Poly(methacrylic acid) – copper ion interactions: phase diagrams: light and X-ray scattering, Polymer 40 (12) (1999) 3331–3344.

[19] J. Blaakmeer, et al., Adsorption of weak polyelectrolytes on highly charged surfaces. Poly (acrylic acid) on polystyrene latex with strong cationic groups, Macromolecules 23 (8) (1990) 2301–2309.

[20] M.J. Zohuriaan-Mehr, K. Kabiri, Superabsorbent polymer materials: a review, Iran. Polym. J. (Engl. Ed.) 17 (6) (2008) 451.

[21] N.M. Hidzir, et al., Radiation-induced grafting of acrylic acid onto expanded poly (tetrafluoroethylene) membranes, Polymer 53 (26) (2012) 6063–6071.

[22] Y. Ma, et al., Porous lignin based poly (acrylic acid)/organo-montmorillonite nanocomposites: swelling behaviors and rapid removal of Pb (II) ions, Polymer 128 (2017) 12–23.

[23] G.R. Mahdavinia, et al., Modified chitosan 4. Superabsorbent hydrogels from poly (acrylic acid-co-acrylamide) grafted chitosan with salt and pH responsiveness properties, Eur. Polym. J. 40 (7) (2004) 1399–1407.

[24] A. Bera, R.K. Misra, S.K. Singh, Structural and behavioral characteristics of radiolytically synthesized polyacrylic acid – polyacrylonitrile copolymeric hydrogels, Radiat. Phys. Chem. 91 (2013) 180–185.

[25] K. Hara, et al., Heavy-metal-cation capturing properties of maleic acid/acrylamide gels, Trans. Mater. Res. Soc. Jpn. 35 (4) (2010) 853–856.

[26] M.B. Huglin, Y. Liu, J. Velada, Thermoreversible swelling behaviour of hydrogels based on N-isopropylacrylamide with acidic comonomers, Polymer 38 (23) (1997) 5785–5791.

[27] J. Mullay, Estimation of Atomic and Group Electronegativities, Springer Berlin Heidelberg, Berlin, Heidelberg, 1987.

[28] B.A. Omondi, et al., Poly (1, 4-diazocane-5, 8-dione) macrocyclic-functionalized hydrogel for high selectivity transition metal ion adsorption, React. Funct. Polym. 125 (2018) 11–19.

[29] A. Sadoc, et al., Structure and stability of VO2+ in aqueous solution: a Car−parrinello and static ab initio study, Inorg. Chem. 46 (12) (2007) 4835–4843.

[30] A. Winston, R.N. Kemper, The split carbonyl band in the infrared spectra of halogen derivatives of 4-hydroxy-2,4-pentadienoic acid lactone, Tetrahedron 27 (3) (1971) 543–548.

[31] N. Sundaraganesan, et al., FT-IR, FT-Raman spectra and ab initio HF and DFT calculations of 4-N,N′-dimethylamino pyridine, Spectrochim. Acta A Mol. Biomol. Spectrosc. 71 (3) (2008) 898–906.

[32] G. Bellucci, et al., Kinetics and mechanism of the reaction of cyclohexene with bromine in the presence of pyridine: competition between different electrophiles, J. Am. Chem. Soc. 102 (25) (1980) 7480–7486.

[33] I.C. McNeill, M. Zulfiqar, Preparation and degradation of salts of poly(methacrylic acid) Part II: magnesium, calcium, strontium and barium salts, Polym. Degrad. Stab. 1 (2) (1979) 89–104.

[34] R. Florin, et al., Factors affecting the thermal stability of polytetrafluoroethylene, J. Res. Natl. Bur. Stand. 53 (2) (1954) 121–130.

[35] M. Szwarc, B. Ghosh, A. Sehon, The C–Br bond dissociation energy in benzyl bromide and allyl bromide, J. Chem. Phys. 18 (9) (1950) 1142–1149.

[36] A. Sehon, M. Szwarc, The C—Br bond dissociation energy in halogenated bromomethanes, Proc. R. Soc. Lond. 209 (1096) (1951) 110–131.

[37] R.S. Urdahl, Y. Bao, W.M. Jackson, An experimental determination of the heat of formation of C2 and the C-H bond dissociation energy in C2H, Chem. Phys. Lett. 178 (4) (1991) 425–428.

[38] K.M. Ervin, et al., Bond strengths of ethylene and acetylene, J. Am. Chem. Soc. 112 (15) (1990) 5750–5759.

[39] X. Yi, et al., Highly efficient removal of uranium (VI) from wastewater by polyacrylic acid hydrogels, RSC Adv. 7 (11) (2017) 6278–6287.

[40] Y. Zhou, et al., Adsorption Behavior of Cd^{2+}, Pb^{2+}, and Ni^{2+} from Aqueous Solutions on Cellulose-Based Hydrogels, vol. 7, 2012, p. 2012.